

Title:

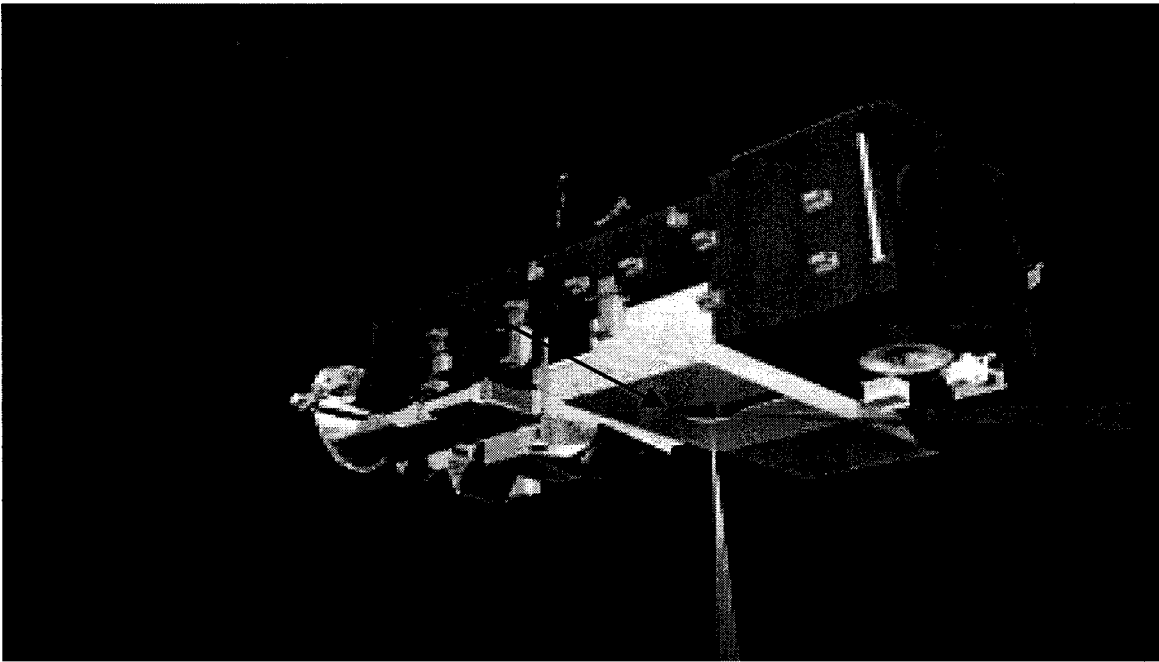
TES Algorithms and Data Products

Authors:

H. Worden, R. Beer, K. Bowman, M. Luo, E. Ustinov
Jet Propulsion Laboratory, California Institute of Technology

S.A. Clough, J. Worden, P. Brown
Atmospheric and Environmental Research, Inc. (AER)

C. Rodgers
Oxford University



The EOS CHEM Tropospheric Emission Spectrometer (TES) Experiment

Global measurements of tropospheric ozone and its precursors from TES combined with *in-situ* data and model predictions will address the following key questions:

How is the increasing ozone abundance in the troposphere affecting

- *climate change?*
- *oxidizing reactions that “cleanse” the atmosphere?*
- *air quality on a global scale?*

TES Standard Products & Required Sensitivity

| Product Name | Product Source | | Required Sensitivity* |
|---|----------------|------|-----------------------|
| | Nadir | Limb | |
| Level 1A Interferograms | ✓ | ✓ | |
| Level 1B Spectral Radiances | ✓ | ✓ | |
| Atmospheric Temperature Profile | ✓ | ✓ | 0.5 K |
| Surface Skin Temperature | ✓ | | 0.5 K |
| Land Surface Emissivity [†] | ✓ | | 0.01 |
| Ozone (O ₃) VMR Profile | ✓ | ✓ | 1 - 20 ppbv |
| Water Vapor (H ₂ O) VMR Profile | ✓ | ✓ | 1 - 200 ppmv |
| Carbon Monoxide (CO) VMR Profile | ✓ | ✓ | 3 - 6 ppbv |
| Methane (CH ₄) VMR Profile | ✓ | ✓ | 14 ppbv |
| Nitric Oxide (NO) VMR Profile | | ✓ | 40 - 80 pptv |
| Nitrogen Dioxide (NO ₂) VMR Profile | | ✓ | 15 - 25 pptv |
| Nitric Acid (HNO ₃) VMR Profile | | ✓ | 1 - 10 pptv |
| Nitrous Oxide (N ₂ O) VMR profile | ✓ | ✓ | Control [‡] |

* Sensitivity range maps to expected concentration range.
NO_x measurements may require averaging to meet these requirements.

[†] Water (and, probably, snow & ice) emissivities are known and are therefore *input*, not output parameters

[‡] Tropospheric concentration known

Potential Special (Research) Products for TES

| Chemical Group | Common Name | Formula | Product Source | |
|-------------------------------|----------------------------|---------------------------------------|----------------|------|
| | | | Nadir | Limb |
| H _x O _y | Hydrogen Peroxide | H ₂ O ₂ | | ✓ |
| | Monodeuterated Water Vapor | HDO | ✓ | ✓ |
| | Ethane | C ₂ H ₆ | | ✓ |
| C-compounds | Acetylene | C ₂ H ₂ | | ✓ |
| | Formic Acid | HCOOH | ✓ | ✓ |
| | Methyl Alcohol | CH ₃ OH | ✓ | ✓ |
| | Peroxyacetyl Nitrate | CH ₃ C(O)OONO ₂ | | ✓ |
| | Acetone | CH ₃ C(O)CH ₃ | | ✓ |
| | Ethylene | C ₂ H ₄ | | ✓ |
| | Peroxynitric Acid | HO ₂ NO ₂ | | ✓ |
| N-compounds | Ammonia | NH ₃ | ✓ * | ✓ |
| | Hydrogen Cyanide | HCN | | ✓ |
| | Dinitrogen Pentoxide | N ₂ O ₅ | | ✓ |
| | Hydrogen Chloride | HCl | ✓ * | |
| Halogen compounds | Chlorine Nitrate | ClONO ₂ | | ✓ |
| | Carbon Tetrachloride | CCl ₄ | | ✓ |
| | CFC-11 | CCl ₃ F | ✓ | ✓ |
| | CFC-12 | CCl ₂ F ₂ | ✓ | ✓ |
| | HCFC-21 | CHCl ₂ F | | ✓ |
| | HCFC-22 | CHClF ₂ | | ✓ |
| | Sulfur Dioxide | SO ₂ | ✓ | ✓ |
| S-compounds | Carbonyl Sulfide | OCS | ✓ | ✓ |
| | Hydrogen Sulfide | H ₂ S | ✓ * | ✓ |
| | Sulfur Hexafluoride | SF ₆ | | ✓ |

* Volcanic/industrial/biomass burning plume column densities only

In order to obtain global coverage of the troposphere for O₃ and its precursors, TES will have the capability of making both limb and nadir observations.

Limb Observations

Advantages

Good vertical resolution.

Enhanced sensitivity for trace constituents.

Disadvantages

Higher probability of cloud interference.

Poorer line-of-sight spatial resolution.

Nadir Observations

Advantages

Lower probability of cloud interference.

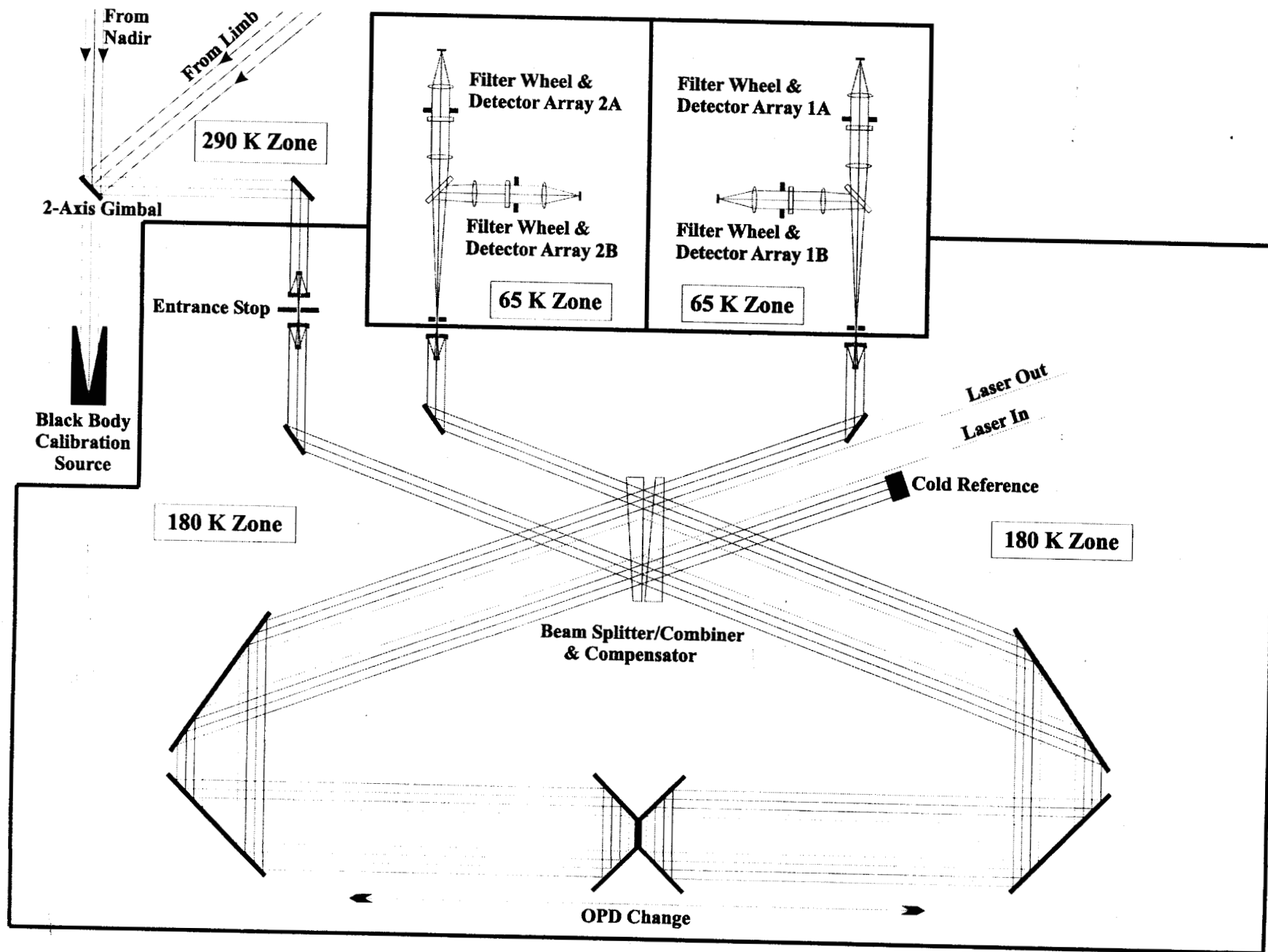
Excellent horizontal spatial resolution.

Disadvantages

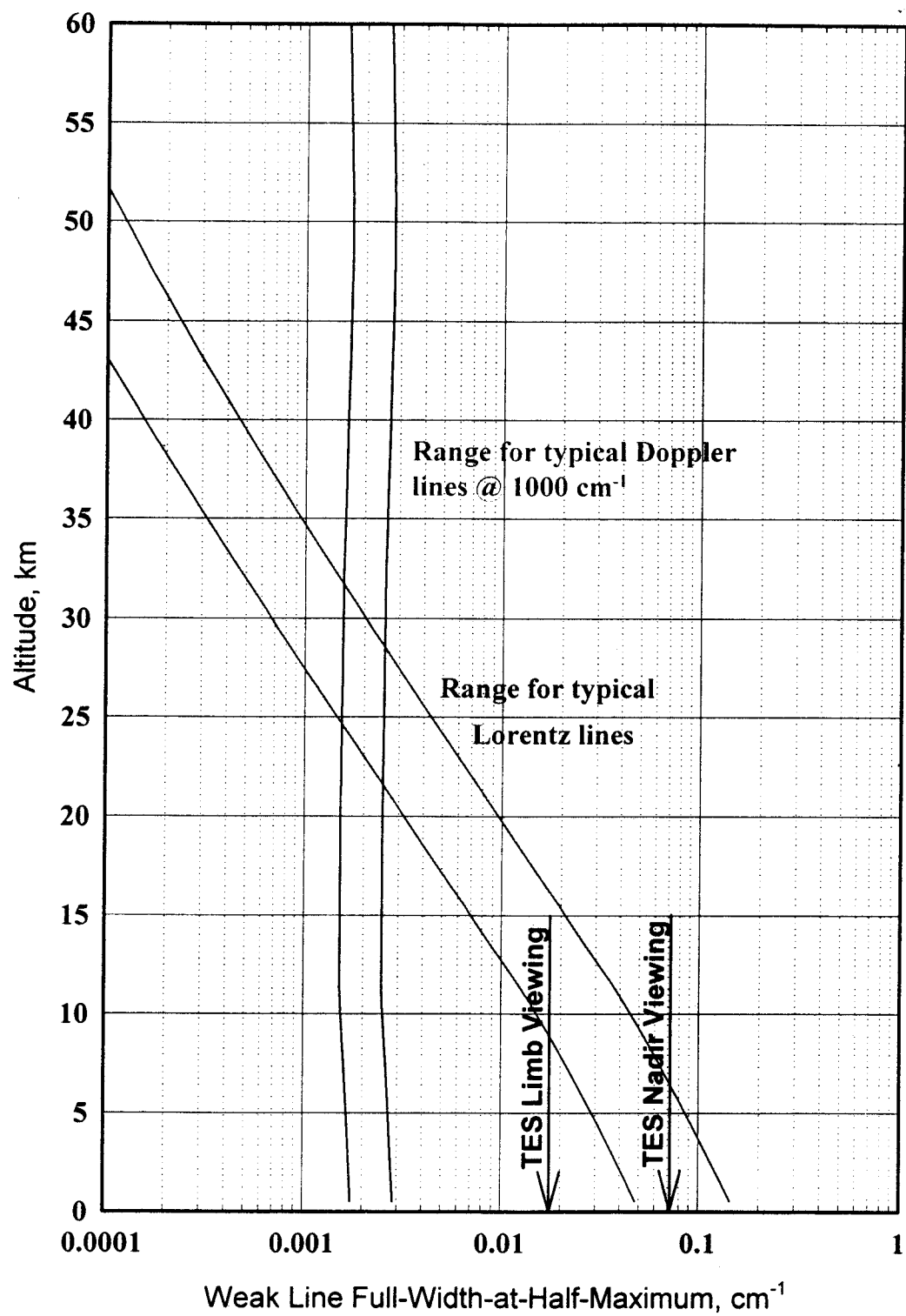
Limited vertical resolution.



TES gimbal pointing mirror



TES Optical Schematic



This figure shows the variation of typical spectral linewidths with altitude. In the lower troposphere, absorption coefficients of pressure broadened lines can be described by the Lorentz function. For higher altitudes, both Doppler and pressure broadening are important, until Doppler broadening dominates at high altitudes. TES spectral resolutions for the nadir and limb views were chosen to match the widths of weak lines in the boundary layer and upper troposphere, respectively.

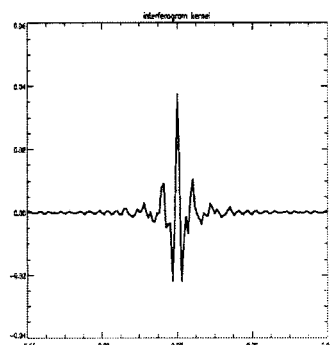
TES Data Processing Steps

Level 1A: Produces geolocated interferograms.

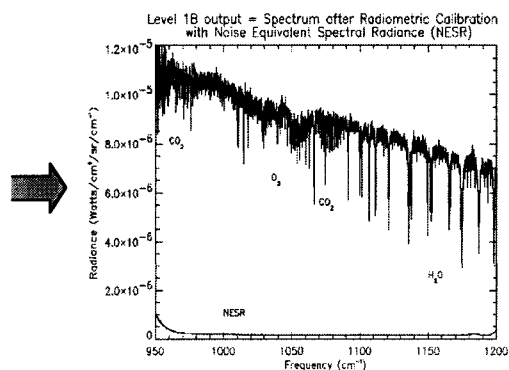
Level 1B: Produces radiometrically and frequency calibrated radiance spectra and estimated NESR (noise equivalent spectral radiance).

Level 2: Produces species abundance and temperature profiles. For cloud-free nadir views, also produces surface temperatures and emissivities.

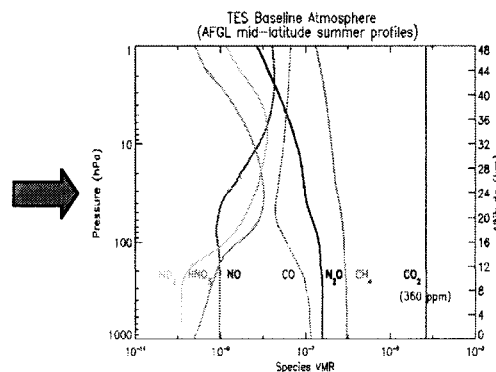
Level 3: Produces global maps for each species at the retrieval pressure levels.



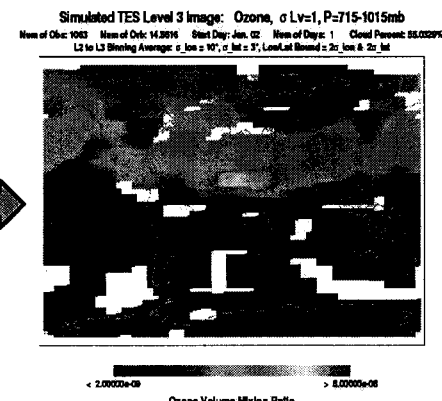
L1A



L1B

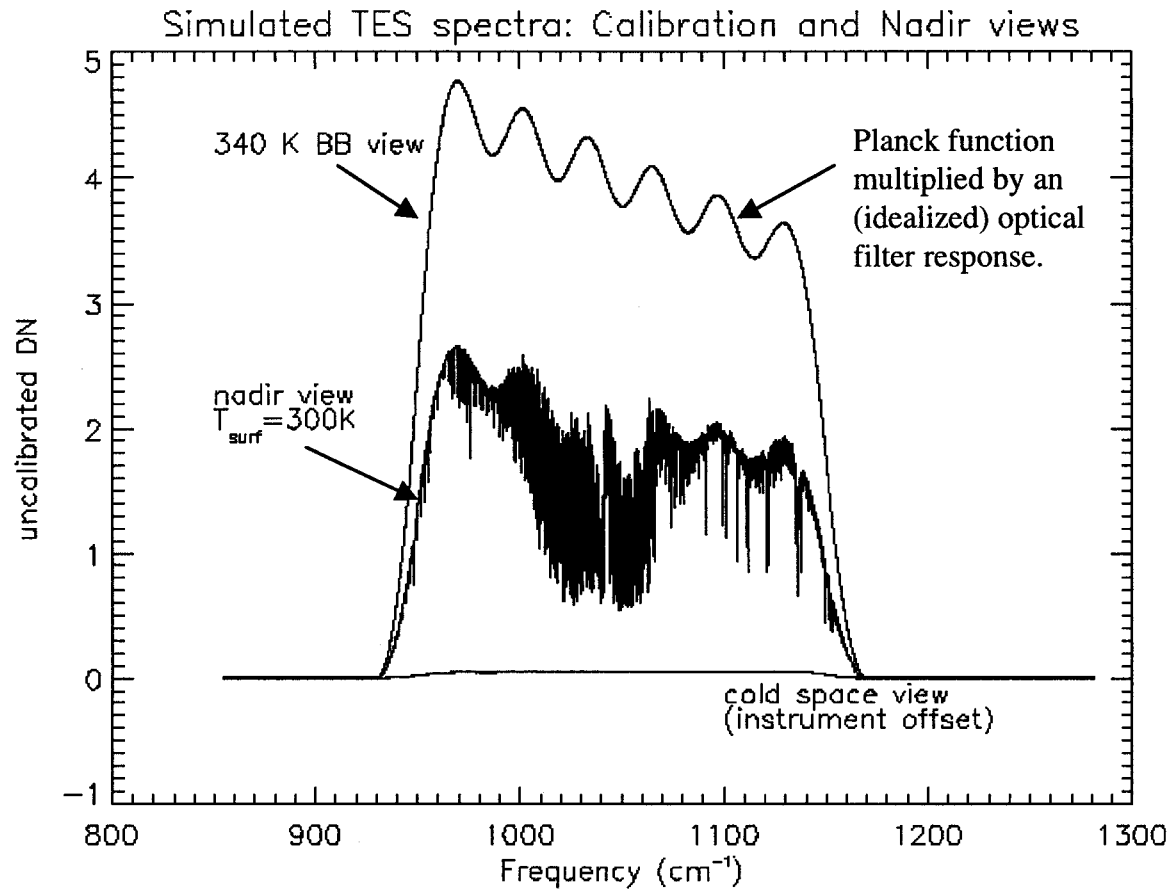


L2



L3

Level 1B Calibration



The complex, uncalibrated measured spectrum is modeled as:

$$C_{\text{target}}(\nu) = r(\nu) [L_{\text{target}}(\nu) + L_{\text{foreoptics}}(\nu) - L_{\text{cold r.p.}}(\nu) + L_{\text{ifmtr}}(\nu) e^{i\phi_{\delta}(\nu)}] e^{i\phi(\nu)} e^{i2\pi m\nu/\nu_1}$$

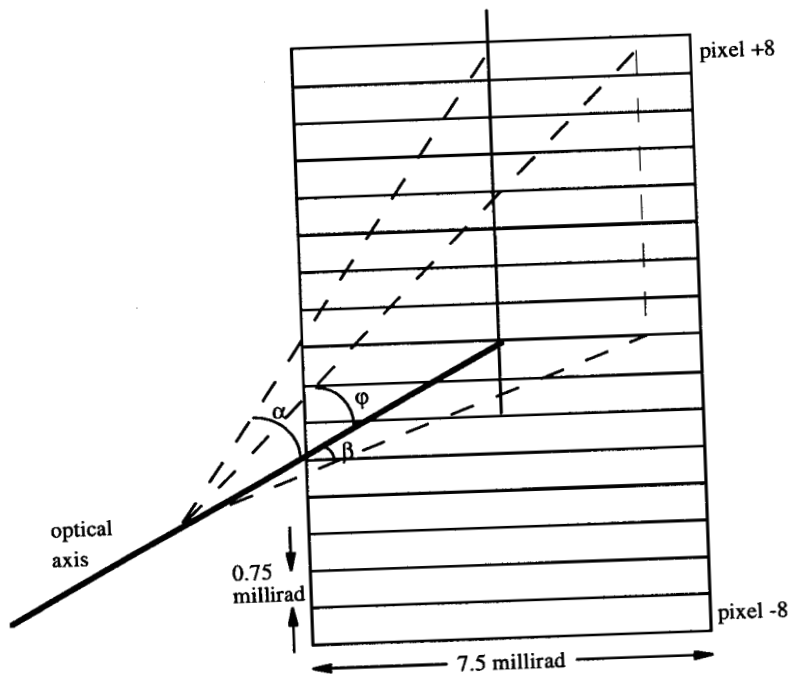
Where the L are source radiance terms, $r(\nu)$ is the instrument response, and the phase terms are separated into 3 contributions: linear sampling phase, $(2\pi m\nu/\nu_1)$, optical and electrical dispersion $(\phi(\nu))$ and the phase difference $(\phi_{\delta}(\nu))$ due to emission within the interferometer (*i.e.*, beamsplitter emission).

Solving for $L_{\text{target}}(\nu)$ using measured calibration spectra C_{BB} & C_{CS} :

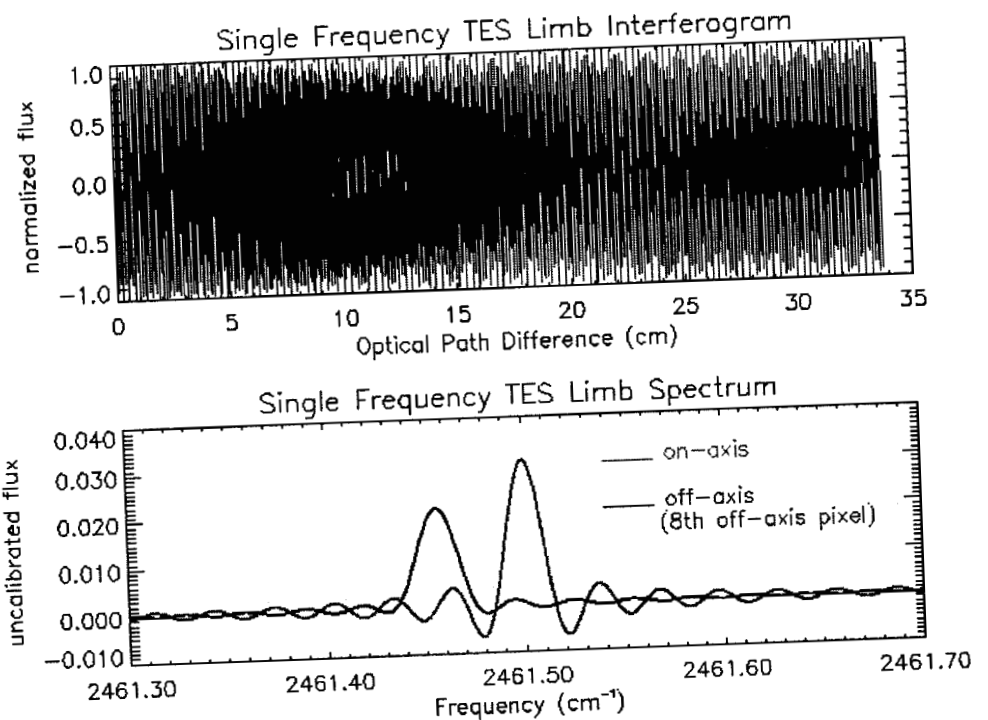
$$L_{\text{target}} = \frac{C_{\text{target}} - C_{\text{CS}}}{C_{\text{BB}} - C_{\text{CS}}} \epsilon_{\text{BB}} B(T_{\text{BB}})$$

Where $B(T_{\text{BB}})$ is the Planck function at the blackbody temperature, ϵ_{BB} is the known blackbody emissivity and we are assuming the cold space (CS) view has negligible source radiance compared to the target, blackbody or the instrument. This also assumes that any time dependence of the terms has been removed (*e.g.* by interpolation) for the times between target and calibration measurements.

Off-axis ILS (Instrument Line Shape) Correction



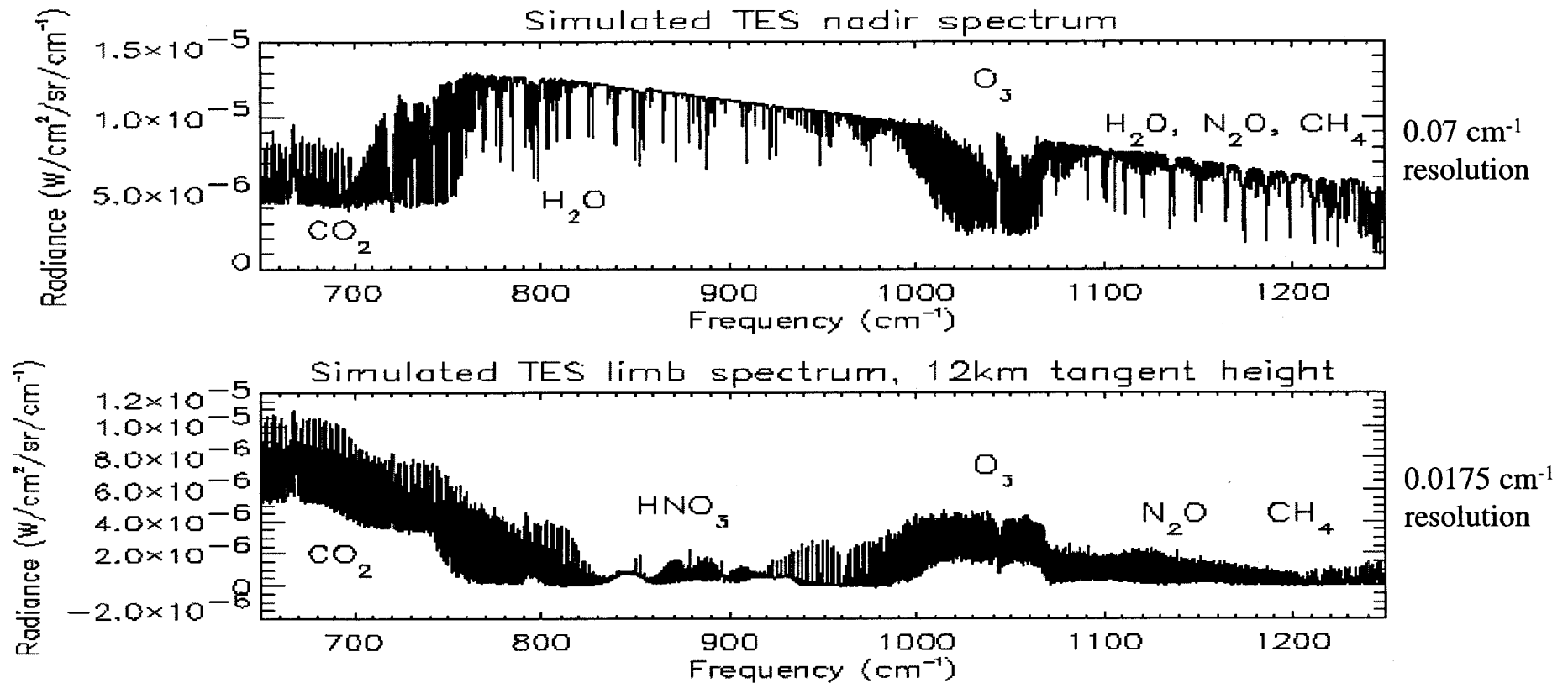
TES pixel array with respect to the optical axis.



Off-axis pixels, as well as the finite field of view (FOV), give rise to frequency scaling, line broadening and line asymmetry compared to an infinitesimal on-axis detector. In order to account for this line shape, we will correct the largest effects in Level 1B and model the remaining asymmetry in Level 2. This approach avoids a costly integration over sub-pixel angles in Level 2 while also allowing us to average nadir spectra before Level 2 retrievals.

Reference: Bowman, *et al.* Instrument line shape modeling and correction for off-axis detectors in Fourier transform spectrometry, *Applied Optics*, accepted for publication, 2000.

Level 1B Products



These spectra are simulated for a mid-latitude summer atmosphere. The estimated NESR (Noise Equivalent Spectral Radiance) is also reported at Level 1B. The NESR is calculated from individual spectra and compared to statistics with measurement ensembles as well as the expected noise performance from the instrument radiometric model.

CLOUDS

Level 1B will determine cloud contamination with different methods to distinguish the following situations:

- 1) Nadir view; partial cloud filling. This type of data would require either an algorithm to extrapolate to a cloud-free radiance or sub-pixel modeling in Level 2 (not currently performed) and is identified by a large scatter in brightness temperatures across the 16 pixels at frequencies where the transmission to the surface is high.
- 2) Nadir and lower limb pixels; cloud filled FOV. This type of data can be used in L2 provided the clouds are opaque. MODIS cloud detection tests [Ackerman *et al.*, 1998] will be adapted for averaged Level 1B spectral channels to determine cloud types. Cloud heights will be estimated by matching the observed brightness temperatures to the temperature fields from current meteorological (*e.g.* ECMWF) data.
- 3) Upper trop. and lower strat. limb pixels. In these cases, the clear-sky background radiance is easier to characterize due to less variability in water vapor. Cloud contamination is determined using seasonal and latitudinal radiance thresholds for high transmission frequency windows. If limb pixels are found to have clouds in the line of sight, only pixels above the highest cloud-contaminated one are used in the L2 retrieval.

MODIS Cloud Detection Groups

| Detection Group | Cloud Types | Detection Technique(s) | MODIS Channels used in Detection |
|-----------------|------------------------------------|---|--------------------------------------|
| I | thick, high clouds (above 500 hPa) | Brightness Temperature (BT) threshold tests for: BT _{13.9} (CO ₂ , 13.9 μm) BT ₁₁ (window region, 11 μm) BT _{6.7} (H ₂ O, 6.7 μm) | 35 31 27 |
| II | thin, high clouds | BT Differences: BT ₁₁ - BT ₁₂ BT _{8.6} - BT ₁₁ BT ₁₁ - BT _{6.7} BT ₁₁ - BT _{3.9} | 31, 32 29, 31 31, 27 31, 21 |
| III | low clouds | (daytime) reflectance ratios and BT differences: BT _{3.9} - BT _{3.7} | 1, 2, 18 21, 20 |
| IV | thin cirrus | (daytime) reflectance threshold test for 1.38 μm | 26 |
| V | thin cirrus | BT Differences: BT _{13.7} - BT _{13.9} BT ₁₁ - BT ₁₂ BT ₁₂ - BT _{3.9} | 34, 35 31, 32 32, 21 |

Compiled from [Akerman, *et al.*, 1998].

| MODIS Channel | Cloud Detection Group(s) | Central Wavelength (μm) | Frequency Range (cm ⁻¹) | TES Filter ID |
|---------------|--------------------------|-------------------------|-------------------------------------|---------------|
| 35 | I, V | 13.94 | 710.0 - 725.4 | 2B1 |
| 34 | V | 13.64 | 725.4 - 741.6 | 2B1 |
| 32 | II, V | 12.02 | 815.0 - 849.6 | 2B1 |
| 31 | I, II, V | 11.03 | 886.5 - 927.6 | 1B1 |
| 29 | II | 8.55 | 1149.4 - 1190.5 | 2A1 |
| 27 | I, II | 6.72 | 1450.3 - 1530.2 | 2A2* |
| 21 | III | 3.96 | 2506.9 - 2545.2 | 1A3* |
| 20 | III | 3.75 | 2604.2 - 2732.2 | 1A4* |

* These filters are not used in the current definition of the Global Survey.

Level 2 Atmospheric Retrievals

Forward Model (FM)

Produces FM Radiance $F(x_i)$ and Jacobian matrix K

Ray Tracing *accounts for atmospheric refraction and geoid.*

Radiative Transfer $F(x_i) = L_{sat} = L_{up} + [\alpha L_{down} + \epsilon B(T_{surface})] \mathcal{T}_{up}$ (clear-sky nadir case)

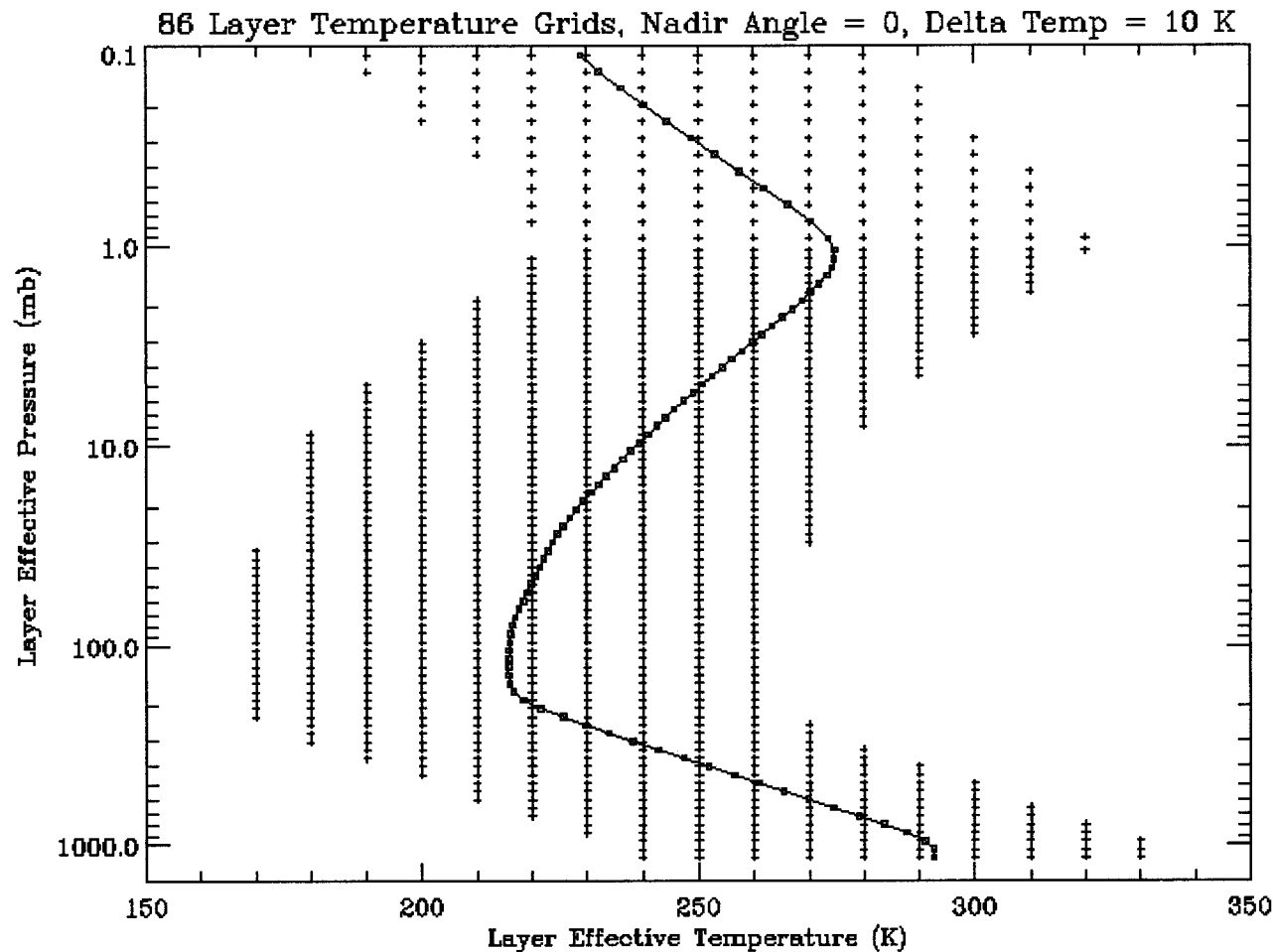
where L_{sat} is the radiance at the satellite, L_{up} , L_{down} are upwelling and downwelling radiances, α and ϵ are the surface albedo and emissivity functions ($\alpha = 1$; $\epsilon = 0$ for the clear-sky limb case) and \mathcal{T}_{up} is the transmission from the surface (or limb tangent point) to the satellite.

- Calculation of optical depths uses tabulated absorption coefficients for line, continua and cross-section species.
- Jacobians are computed analytically.

ILS Convolution *monochromatic grid (nominally 0.0002 cm^{-1}) is convolved with the instrument line function (ILS) which is a sinc function combined with the complex off-axis asymmetry function in interferogram space.*

FOV Convolution (limb case only) *Uses measured detector angular response functions.*

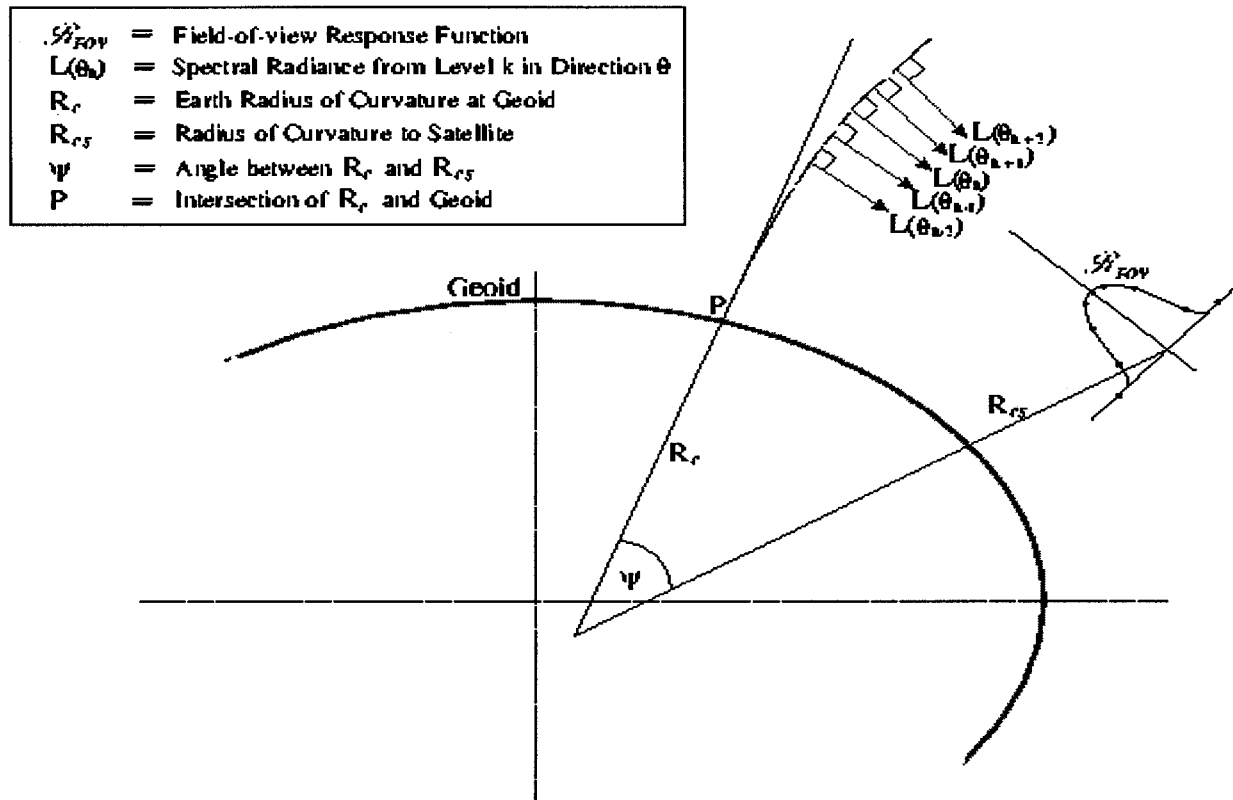
Pressure-Temperature Grid for Tabulated Absorption Coefficients



This plot shows the vertical levels and temperature values for which absorption coefficients are calculated, with a global, seasonal average temperature profile overplotted. Line absorption is calculated using the LBLRTM code (Clough & Iacono, 1995) with the HITRAN molecular database (Rothman, et al., 1992). Radiative transfer calculations will be performed on either a sub-set or the full 86 layers shown above, depending on the accuracy required.

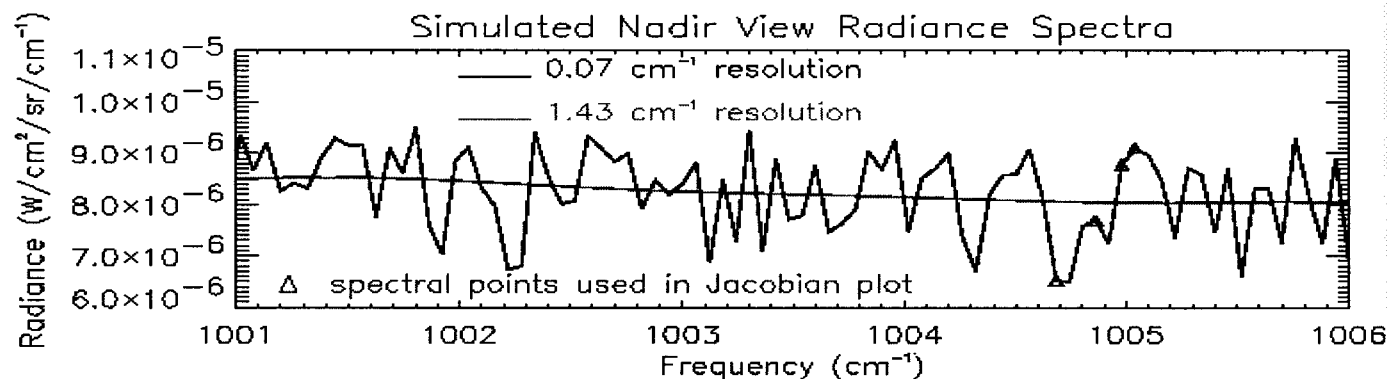
References: Clough, S.A. and M.J. Iacono, *JGR*, 100, 16519-16535, 1995; Rothman, L.S. *et al.*, *JQSRT*, 48, 469-507, 1992.

Limb FOV (field of view) Convolution



This figure illustrates the FOV convolution for a single limb viewing pixel. For 16 pixels in each detector array, 33 individual rays (about 1.2 km apart) must be computed and convolved with \mathcal{R}_{FOV} to accurately model the radiance gradients in the limb view.

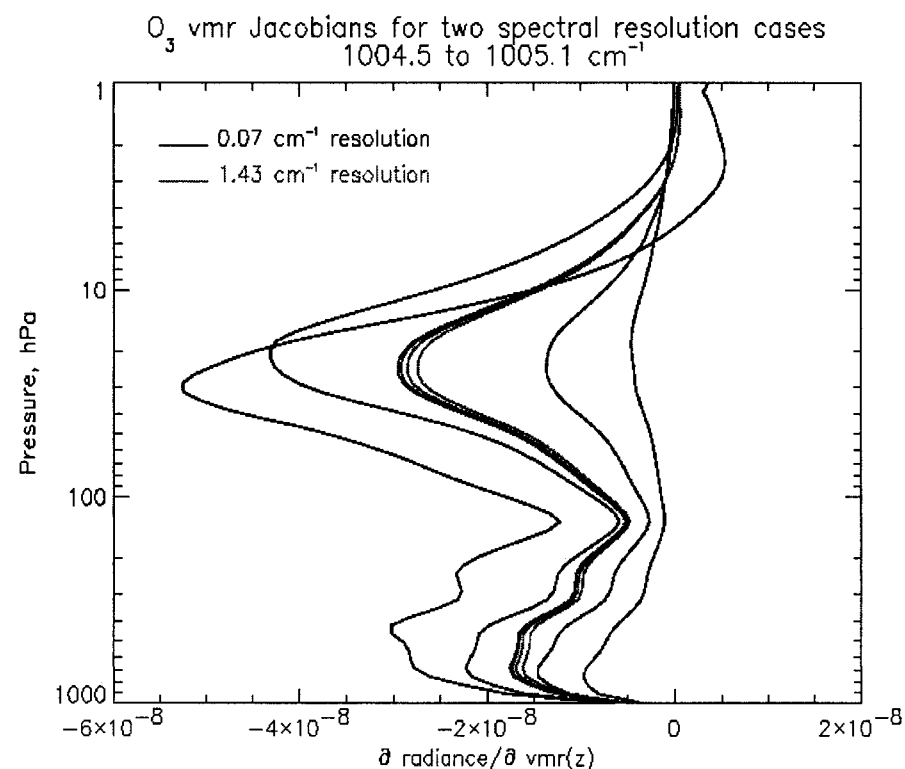
Nadir spectral resolution and vertical sensitivity



TES spectral resolution for the nadir view (0.07 cm^{-1}) was chosen to match pressure-broadened weak lines in the lower atmosphere.

O₃ vmr Jacobians are a measure of the sensitivity of the radiance measurement to a change in the O₃ abundance at each altitude. This plot shows how spectral points along an absorption feature have different inherent vertical information for the TES nadir resolution case (0.07 cm^{-1}). For the 0.07 cm^{-1} resolution case, the peaks in the Jacobians occur at different pressure levels, in both the strat & trop, for different spectral positions, while there is almost no variation in the degraded resolution case. Also, the TES resolution case has much greater variation in the ratios of stratospheric and tropospheric sensitivity peaks.

Note that this study does not address issues of relative SNR between the resolution cases, since noise in the measurements does not change the Jacobian calculation.



Inversion

estimates atmospheric and surface parameters by minimizing the cost function:

$$[y - F(x)]^T S_e^{-1} [y - F(x)] + [x - x_a]^T S_a^{-1} [x - x_a]$$

where y is the measured spectrum, S_e is the measurement covariance, x is the state vector of atmospheric parameters, x_a is the a priori state vector and S_a is the a priori covariance.

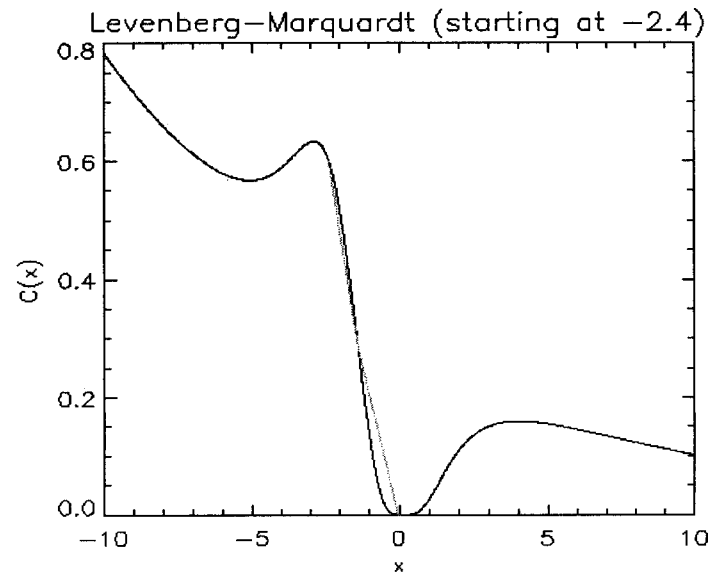
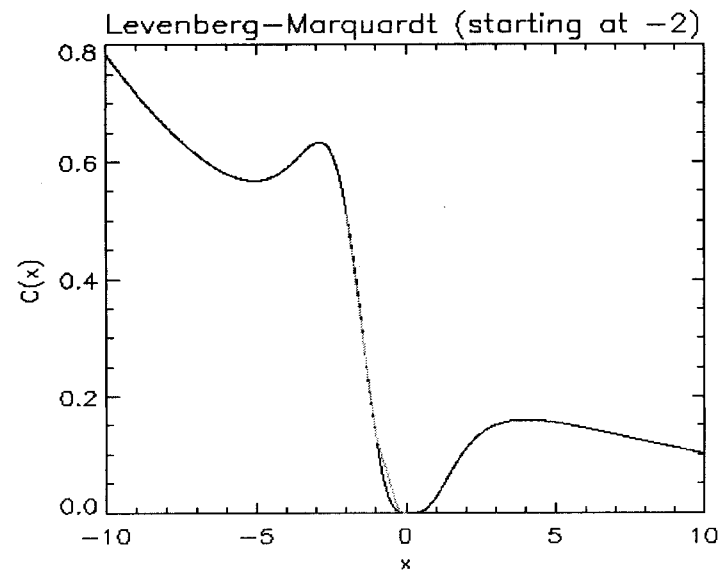
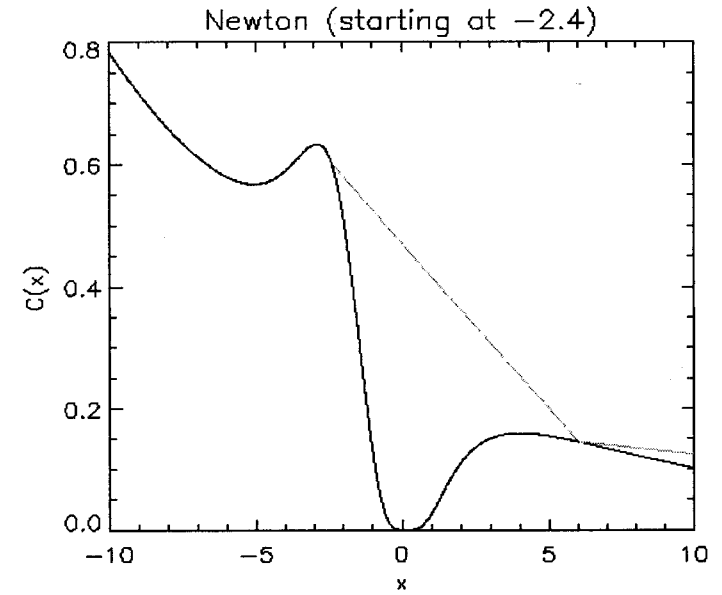
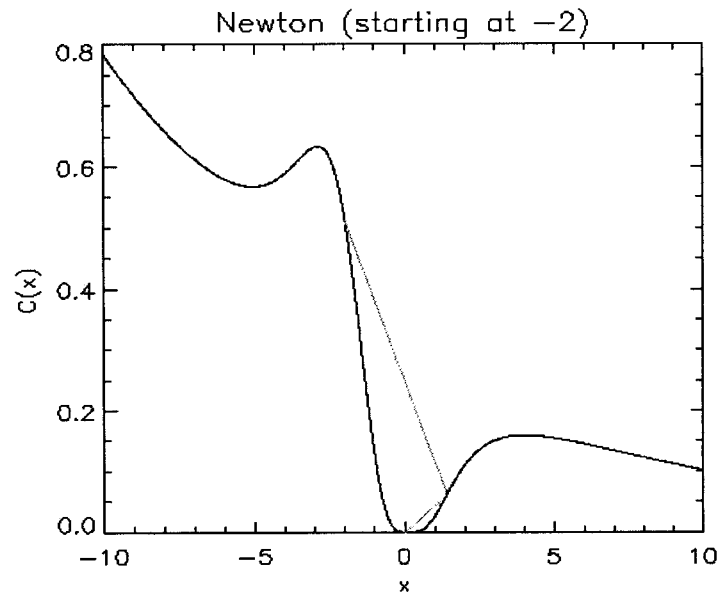
Cost function *algorithm uses either the first term only: maximum likelihood (ML)
or both terms: maximum a posteriori (MAP)*

Iteration step $x_{i+1} = x_i + (K^T S_e^{-1} K + S_a^{-1} + \gamma)^{-1} (K^T S_e^{-1} [y - F(x_i)] - S_a^{-1} [x_i - x_a])$

*either Gauss-Newton ($\gamma = 0$; small residual case, i.e., good initial guess)
or Levenberg-Marquardt ($\gamma > 0$; non-linear regimes - slower but more robust)*

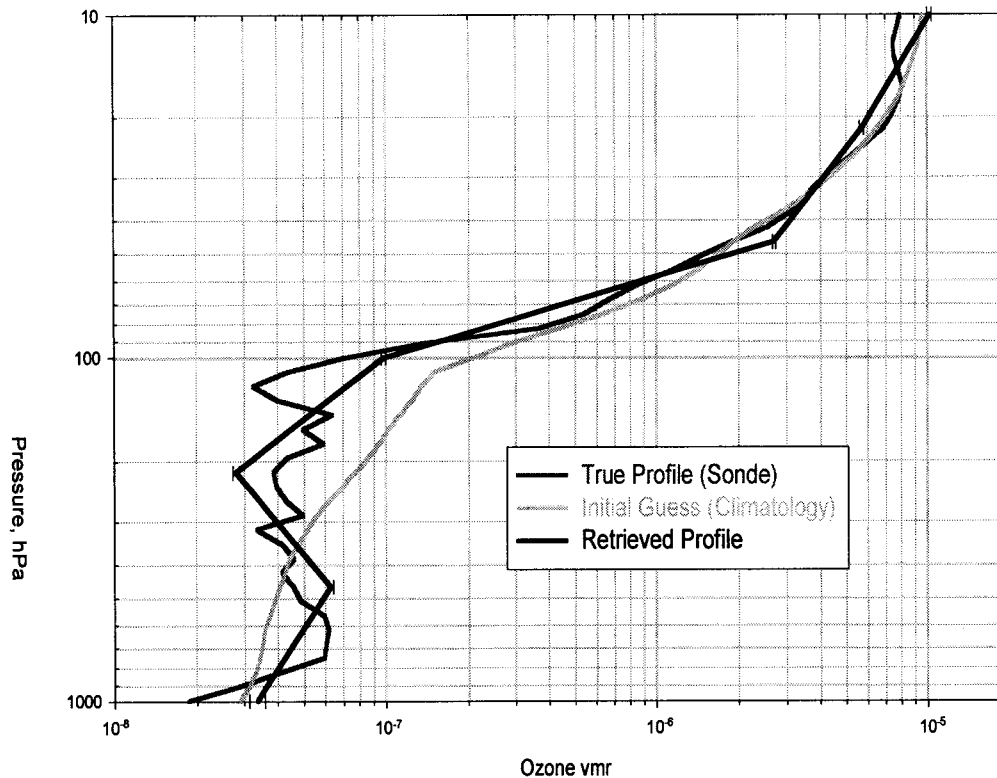
Convergence *first term of cost function reaches estimated measurement noise variance.*

1-D Example of Gauss-Newton vs. Levenberg-Marquardt Steps



TES nadir O₃ retrieval example

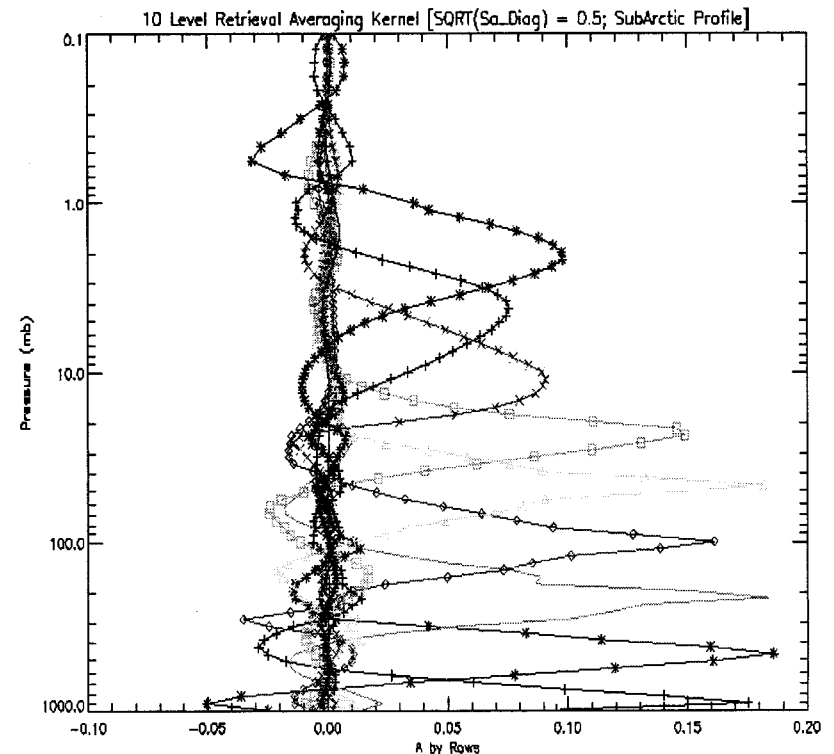
Top left: retrieved profile compared to the true profile used in the simulated input spectrum and the initial guess profile used as the retrieval starting point.



Bottom right: Averaging (A) kernel for a TES nadir O₃ retrieval.

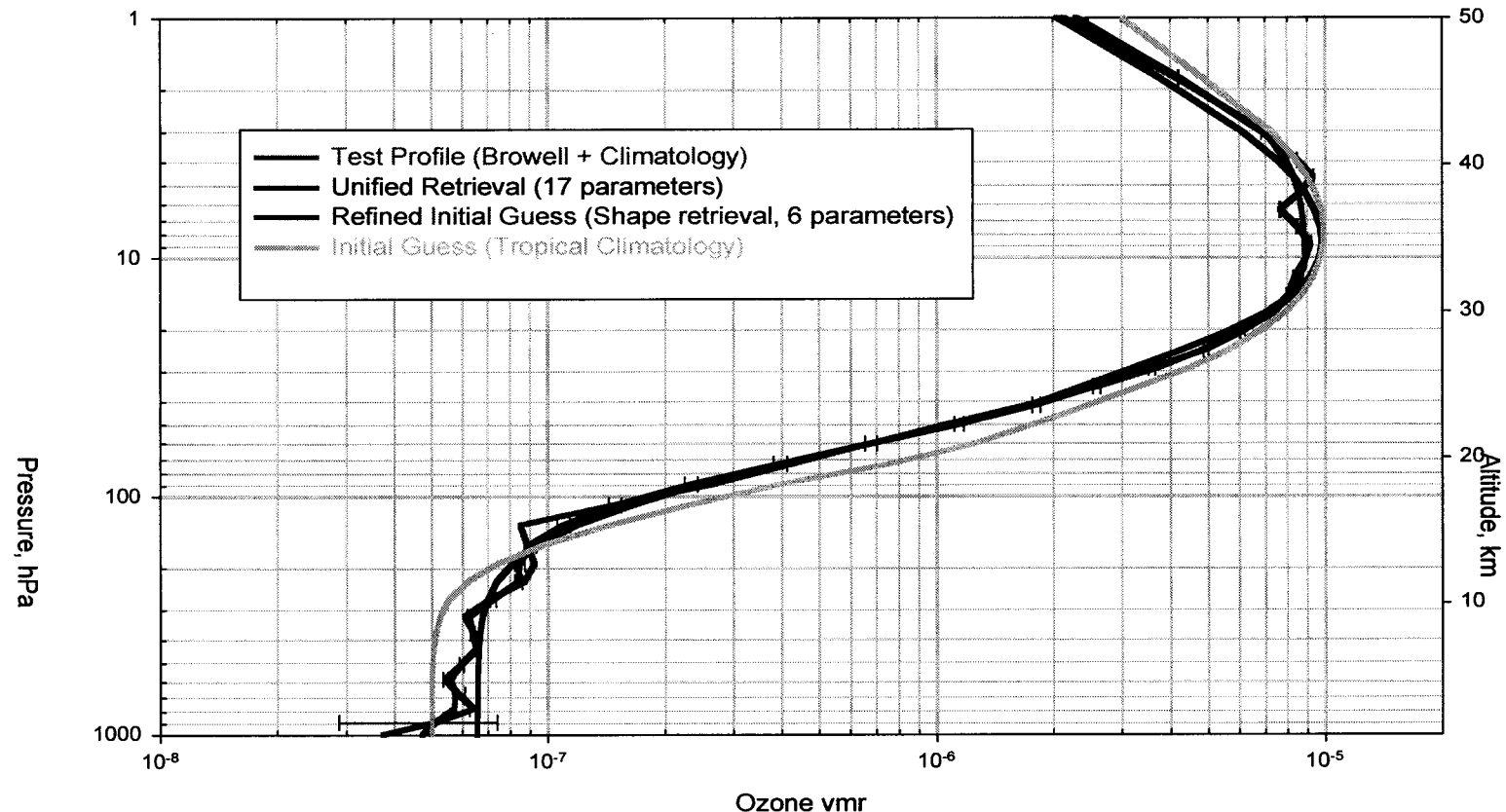
$$A = (K^T S_e^{-1} K + S_a^{-1})^{-1} K^T S_e^{-1} K$$

Rows of A are plotted to show the expected vertical resolution (estimated by the FWHM of the peaks) as a function of pressure level.



Reference: Clough, *et al.*, Retrieval of tropospheric ozone from simulations of nadir spectral radiances as observed from space, *JGR* 100, 16579-16593, 1995.

TES limb O₃ retrieval example



In some cases, TES retrievals will use a “shape retrieval” as an initial guess refinement step. This allows a quick (single iteration) retrieval of a few shape parameters to obtain a smooth profile that is closer to the true profile than the available first guess. In this case, the initial guess (green) was a factor of 2 different in the lower stratosphere. The final retrieval on 17 pressure levels to obtain vertical structure in the tropospheric profile also converged in a single iteration for the case shown.

Level 2 Products

Standard Products

- Profiles of O_3 , H_2O , CO , CH_4 , NO , NO_2 , HNO_3 VMR and atmospheric temperature (T) on a subset of the UARS pressure levels; Nadir T_{surface}

- Associated with each profile:

1σ statistical errors (square root of diagonal of $S_x = (K^T S_e^{-1} K + S_a^{-1})^{-1}$)
estimated systematic error

Fraction of Explained Variance $FEV = 1 - (S_x)_{ii}(S_a^{-1})_{ii}$

This is a measure of the relative weights of measurement and *a priori* to the retrieved parameter, *i.e.*, $FEV = 1$ implies that all the information came from the measurement; $FEV = 0$ implies that only the *a priori* contributed to the retrieved value.

Correlation distance $Z_{corr}(x_i, x_j) = -\Delta z / \ln(|\rho_{ij}|)$

where Δz is the vertical separation of parameters x_i and x_j and ρ_{ij} is the correlation between them: $\rho_{ij} = (S_x)_{ij} / [(S_x)_{ii}(S_x)_{jj}]^{1/2}$. May report only max and mean values; separated trop & strat.

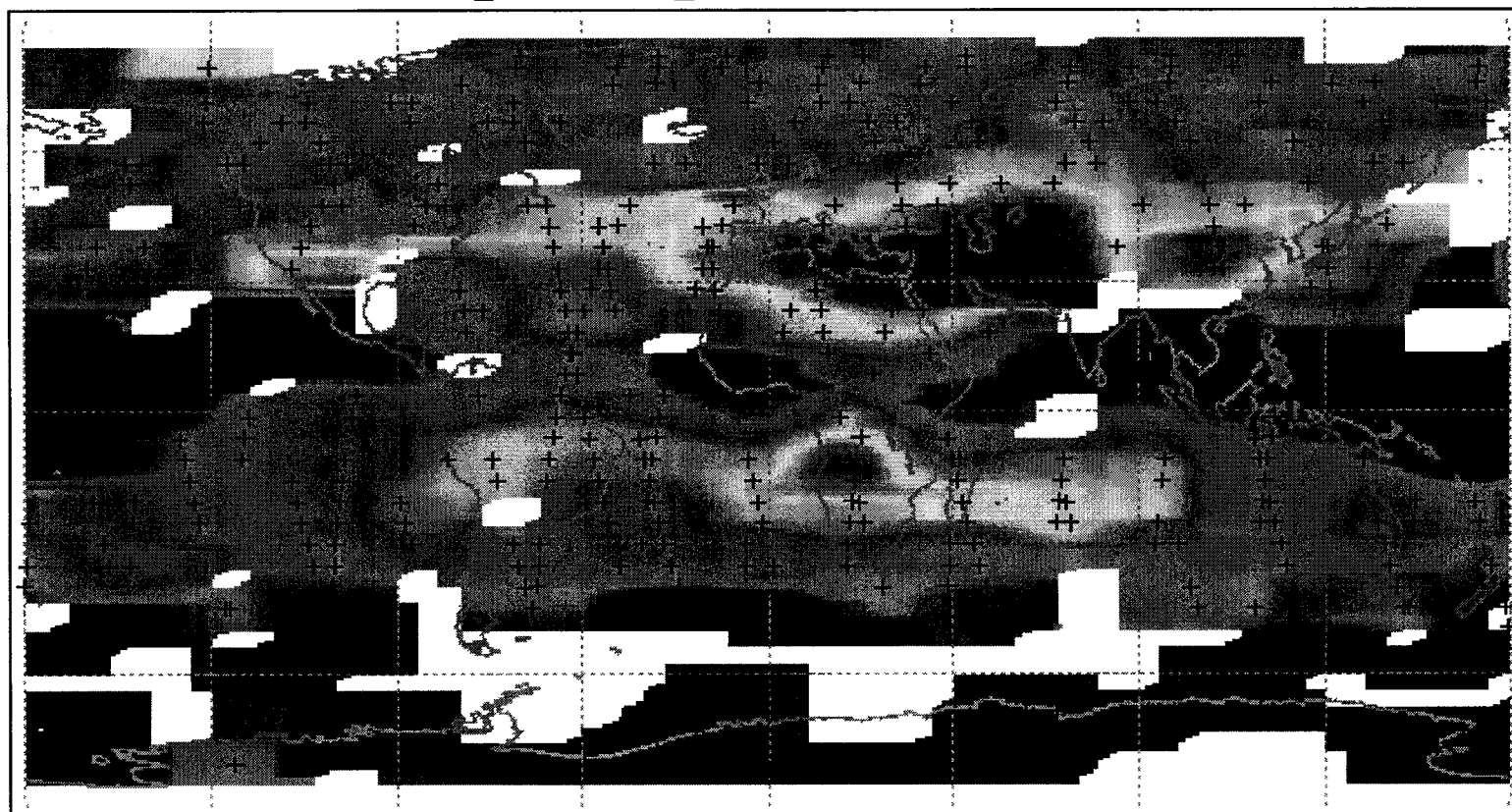
Standard Diagnostic Products

- Full Covariance Matrix S_x
- Residuals (Data - Model difference) for entire measured spectrum
- For Nadir observations over land, surface emissivities (coarse frequency grid).
- For Limb observations, microwindow smooth background parameters (non-zero values may indicate the presence of aerosols or thin clouds.)

Level 3 Global Maps

Simulated TES Level 3 Image: Ozone, P = 464.2 hPa

Num of Obs: 476/1063 Num of Orb: 14.56 Start Day: Aug. 15 Num of Days: 1 Total Cloud Percent: 55.2%
L2 to L3 Bin Ave: $\sigma_{lon} = 10.0^\circ$, $\sigma_{lat} = 3.0^\circ$, Lon/Lat Bound = $2\sigma_{lon}$ & $2\sigma_{lat}$



< 2.00e-08

> 7.50e-08

Ozone Volume Mixing Ratio

The above map shows a simulated, smoothed L3 image and the corresponding single point nadir observations (for 1 day) after accounting for drop-outs due to clouds. The O₃ amounts are from sampling the Harvard-GEOS model at the planned TES nadir observation spacing.

References: http://www-as.harvard.edu/chemistry/trop/geos/geos_model.html

TES In-flight Data and Algorithm Self-consistency Tests

Level 1B

Calibration test using the on-board blackbody allows a check of both the calibration system and algorithm, *i.e.*, the calibration of a blackbody interferogram (for the blackbody at any temperature) must produce the known blackbody radiance.

Level 2

- TES can measure the same species in different spectral windows and can check that retrieved amounts are the same.
- Residuals in H₂O lines using the initial retrieved temperature profile are a check on the temperature retrieval.
- After the final L2 iteration, residuals will be calculated for the entire measured spectrum (not just microwindows) to check for retrieval errors as well as to search for unmodeled atmospheric constituents.